AJNR Am J Neuroradiol 21:151–158, January 2000

Phase-Contrast MR Imaging of the Cervical CSF and Spinal Cord: Volumetric Motion Analysis in Patients with Chiari I Malformation

Erich Hofmann, Monika Warmuth-Metz, Martin Bendszus, and Lászlò Solymosi

BACKGROUND AND PURPOSE: **Most previous MR studies of the dynamics of Chiari I malformation have been confined to sagittal images and operator-dependent measurement points in the midline. To obtain a deeper insight into the pathophysiology of the Chiari I malformation, we performed a prospective study using axial slices at the level of C2 to analyze volumetric motion data of the spinal cord and CSF over the whole cross-sectional area.**

METHODS: **Eighteen patients with Chiari I malformation and 18 healthy control subjects underwent cardiac-gated phase-contrast imaging. Cross-sectional area measurements and volumetric flow/motion data calculations were made for the following compartments: the entire intradural space, the spinal cord, and the anterior and posterior subarachnoid space.**

RESULTS: **The most striking feature was an increased early systolic caudal and diastolic cranial motion of the spinal cord in the patients. CSF pulsations in the anterior subarachnoid space were unchanged at systole but showed an impaired diastolic upward flow. In the posterior compartment, the CSF systole was slightly shortened, with an impairment of diastolic upward flow. Fourteen of the 18 patients had associated syringeal cavities. This subgroup showed an increased systolic downward displacement of the cord as compared with patients without a syrinx.**

CONCLUSION: **Obstruction of the foramen magnum in patients with Chiari I malformation causes an abrupt systolic downward displacement of the spinal cord and impairs the recoil of CSF during diastole.**

Several MR studies have analyzed the changes in CSF and brain pulsations in patients with Chiari I malformation. Most previous investigators have used midsagittal sections. Motion has been encoded using either the phase-contrast technique (1–4) or presaturation bolus tracking (5). Similar measurements in the axial projection have been limited (6). Although the quantitative data from sagittal images are consistent and considered valid (2), the selection of measuring points, and hence the results, are operator-dependent. Furthermore, the quantification of in-plane flow using the phase-contrast technique is hampered by partial volume effects and, as a result, can give false measurements. Another shortcoming of this imaging geometry is its confinement to the midsagittal plane, which leaves flow and motion in the lateral compartments and their implications undetected or necessitates additional lateral studies. A more pathophysiologically related description would require a motion analysis of isolated compartments, and it was for this reason that we undertook the present prospective study. Our purpose was to quantify the volumetric motion of the spinal cord and cervical CSF space in patients with Chiari I malformation and to find consistent differences in CSF flow and cord motion in comparison with normal findings.

Received January 21, 1999; accepted after revision August 18, 1999.

From the Department of Neuroradiology, University of Würzburg, Germany.

Address reprint requests to PD Dr. E. Hofmann, Department of Neuroradiology, University of Würzburg, Josef-Schneider-Str. 11, D-97080 Würzburg, Germany.

Methods

Patients and Control Subjects

We carried out a prospective study of 18 consecutive patients (eight male and 10 female; 3 to 79 years old; mean age, 35 ± 22 years), all of whom fulfilled the diagnostic criteria (7, 8) of Chiari I malformation, with their tonsillar tip lower than −5 mm below the basion-opisthion line, as determined on the basis of T1-weighted sagittal MR images. The patients underwent imaging for symptoms that could be attributed to Chiari I malformation itself (cough-strain headache, vestibular symptoms) or to associated syringomyelia (gait problems, paresthesia, sensory deficits). The findings in the patients were compared with those in 18 healthy volunteers with a compa-

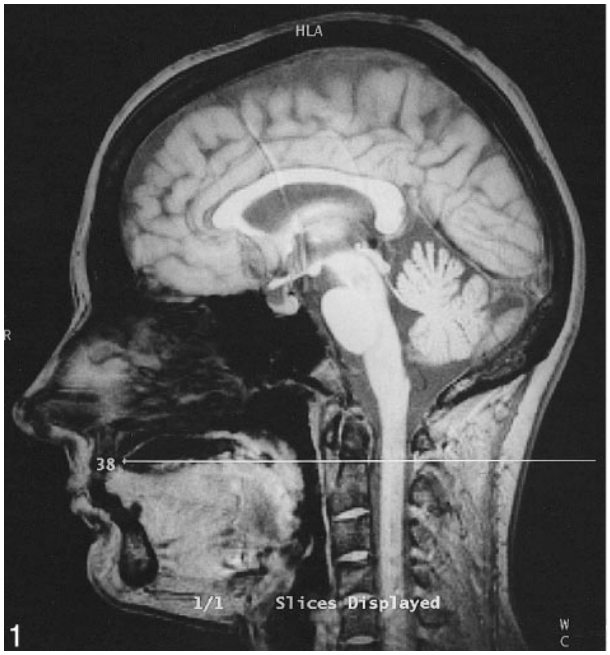

FIG. 1. Sagittal reference image with axial section perpendicular to the spinal canal at the level of C2.

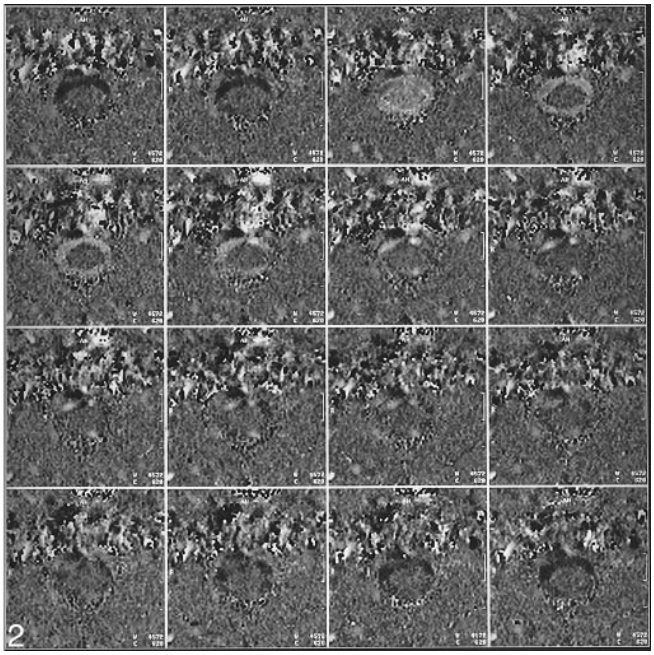

FIG. 2. Phase-contrast images (partitions 1 through 16) corresponding to Figure 1.

rable age and sex distribution (nine male and nine female subjects; 10 to 62 years old; mean age, 37 ± 14 years). The control subjects were without any history of neurologic disease and had no neurologic symptoms. The volunteer studies were performed after informed consent had been obtained.

Imaging Protocol

Examinations of the patients and control subjects were performed with a 1.5-T imager and with the use of a commercially available phase-contrast flow quantification sequence: flip angle (α), 30°; TR/TE, 60/5; slice thickness, 5 mm; field of view, 180 mm; matrix, 256 × 256; encoding velocity (v_{enc}), 10 cm/s. Slice orientation was perpendicular to the spinal canal, slice position was chosen at the level of the body of the axis (Fig 1). Electrocardiographic (ECG) triggering was performed prospectively with 16 equidistant image frames. The trigger impulse (R wave) was obtained using MR-compatible chest electrodes. The TR of the whole sequence was set approximately 5 minutes after the patient or volunteer had entered the scanner and had become familiar with the environment, thus enabling each subject to adjust to her or his resting heartbeat frequency. As the TR of the whole sequence was exactly the same as the actual heartbeat interval, the 16 partitions covered the whole cardiac cycle, leaving no ''dead zone'' at the end of diastole. Physiologic heart frequency fluctuations meant that a significant proportion of R waves had to be rejected if the actual R-R interval was shorter than the overall TR; nevertheless, this time penalty was accepted in the interest of full coverage of the cardiac cycle. Retrospective triggering was not available with the sequence chosen. The number of partitions (1–16) was expressed in terms of a percentage fraction of the complete cardiac cycle. This normalization of temporal data against the heartbeat interval permitted a comparison of subjects and groups with different heart rates. A typical set of partitions is shown in Figure 2. Velocity encoding was cranial to caudal. By convention, caudal flow or motion was designated hyperintense and cranial motion hypointense. Stationary tissue was depicted as gray. By using a v_{enc} of 10 cm/s, there was no aliasing. A lower v_{enc} would have been desirable to measure slow motion more accurately, but was not available when we started our study. On the other hand, in a previous sagittal study, researchers had observed aliasing even with a v_{enc} of 5 cm/s (4). Another shortcoming of our sequence was the relatively low temporal sampling resolution, which was on the order of 60 milliseconds, thereby limiting the accuracy of cord motion measurements.

Flow Rate Analysis

All the flow images were evaluated using the image analysis software installed in the scanner's operator console. An irregular region of interest (ROI) was drawn manually to encompass the cross-sectional area of the entire intradural compartment, the spinal cord, and the posterior subarachnoid space. Care was taken not to include the epidural space. The spinal cord was best outlined in early systole, when the contrast between CSF and cord was at its maximum. In patients with a high cervical syrinx, the cavity was included in the cord area. Offsets of the zero-velocity baselines due to eddy currents and residual phase shifts had to be compensated. To do this, the offset velocity was estimated on a frame-by-frame basis using stationary tissue (the inferior obliquus capitis muscle) as a reference. Velocities were corrected by subtracting this background velocity from every partition. A multiplication of flow velocities with the relevant cross-sectional areas resulted in volumetric flow rates. The volumetric flow rates of the anterior CSF were obtained by subtracting the spinal cord flow rates from those of the whole intradural compartment and by subtracting from this entire CSF space the flow rates of the posterior CSF space.

Experimental studies using a flow phantom with tubes of various diameters (1, 2, 3, and 6 mm) and constant flow had demonstrated a good linear correlation ($r = .93$, $P < .0001$) between true flow rates and measurement values, irrespective of tube diameters, with only a linear correction factor being necessary.

The flow rates were expressed as mean values for the corresponding subgroup. They were plotted on the *y*-axis, and the temporal partitions (as a percentage of the cardiac cycle) were plotted on the *x*-axis. After 16 partitions, the cycle started again with partition 1 of the new cycle. The craniocaudal flow rates corresponding to the CSF systole are depicted as negative values, and caudocranial diastolic flow rates as positive values.

TABLE 1: Comparison of area measurements between control subjects and patients

Area	Control Subjects	Patients	Difference
Intradural space	3.2 ± 0.5 cm^2	3.5 ± 1.3 cm^2	N.S.
Spinal cord	0.9 ± 0.1 cm^2	1.2 ± 0.4 cm^2	N.S.
Anterior CSF	1.0 ± 0.3 cm^2	1.1 ± 0.6 cm^2	N.S.
Posterior CSF	1.3 ± 0.4 cm^2	1.3 ± 0.6 cm^2	N.S.

Note.—N.S. indicates no significant difference.

The statistical significance of the measurements and of the biographical data was calculated by means of a nonparametric test (Wilcoxon test). Significant differences were assumed when *P* was less than .01. Sex distribution among the patients and control subjects was assessed using Fisher's exact test.

Results

The tonsillar position in patients varied considerably, ranging from −6 mm to −29 mm below the basion-opisthion line (mean, −12.9 ± 5.9 mm; median, −11 mm). None of the control subjects had caudal dystopia of the cerebellar tonsils. Eleven (61%) of the 18 patients had a cervical syringomyelia that expanded the cord, three (17%) had a nonexpanding syrinx. No patient had been operated on or had hydrocephalus. Table 1 shows the planimetric results for patients and control subjects. On average, the patients tended to have a larger cross-sectional area of both the cord and intradural compartment as a whole, although the differences failed to reach significance. Table 2 gives the maximum systolic and diastolic flow rates for the various compartments. The most striking finding was the significantly increased maxima for the systolic and diastolic volumetric motion rate of the cord in the patients. Figure 3 depicts the flow rates for the entire intradural compartment in patients and control subjects. The flow rates followed an approximately sinusoidal pattern. At no heart phase was there a significant difference between the patients and control subjects.

The flow rates of the anterior (Fig 4) and posterior (Fig 5) CSF showed a similar pattern. The patients, however, had a delayed return to diastolic upward flow in the anterior CSF with some overshoot at late diastole. The CSF systole in patients was slightly shorter and less marked in the posterior CSF compartment, and diastolic upward flow was also impaired. When the anterior and posterior compartments are taken together, the patients showed a significant impairment of upward flow from frame 11 to 13 (63% to 75% of the cardiac cycle, data not shown).

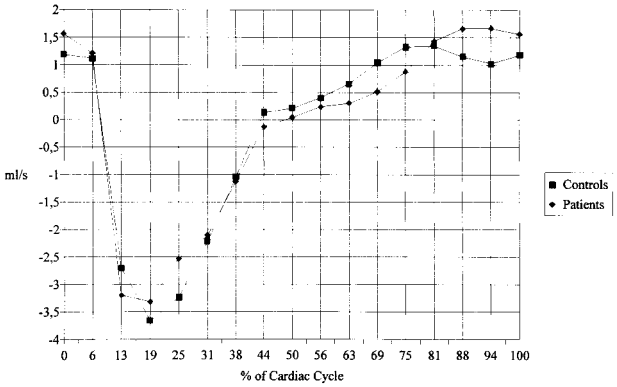

FIG. 3. Volumetric motion (mean values) of the upper cervical intradural space as a whole. There are no significant differences between patients and control subjects.

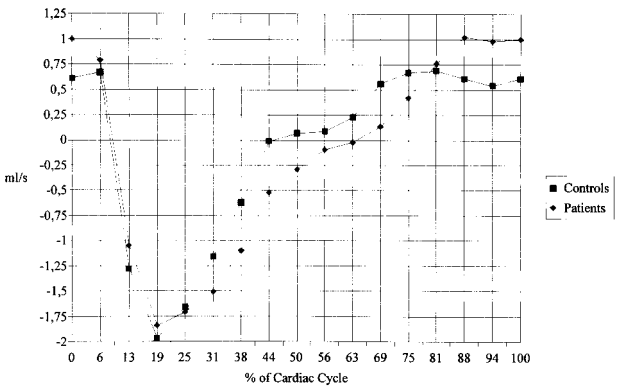

FIG. 4. Flow rates (mean values) of anterior cervical CSF motion. Significant differences are seen between patients and control subjects at 0%, 44%, and 69% of the cardiac cycle.

Figure 6 shows a similar temporal pattern of cord motion in patients and control subjects. In general, the motion pattern was less sinusoidal than in CSF but appears to be superimposed by higher-order oscillations. Early in systole, the short downward displacement of the cord tended to be faster in patients than in control subjects. At diastole, the upward

TABLE 2: Comparison of maximum volumetric flow and motion rates between control subjects and patients

Area	Control Subjects	Patients	Difference
Intradural space, systole	−4.7 ± 2.0 mL/s	−4.3 ± 1.6 mL/s	N.S.
Spinal cord, systole	−0.5 ± 0.2 mL/s	−0.9 ± 0.6 mL/s	$P < .01$
Anterior CSF, systole	−2.4 ± 1.4 mL/s	−2.2 ± 0.9 mL/s	N.S.
Posterior CSF, systole	−1.9 ± 0.9 mL/s	−1.8 ± 1.0 mL/s	N.S.
Intradural space, diastole	2.0 ± 0.8 mL/s	2.2 ± 1.0 mL/s	N.S.
Spinal cord, diastole	0.2 ± 0.1 mL/s	0.4 ± 0.3 mL/s	$P < .01$
Anterior CSF, diastole	1.1 ± 0.5 mL/s	1.3 ± 0.6 mL/s	N.S.
Posterior CSF, diastole	0.9 ± 0.4 mL/s	0.8 ± 0.4 mL/s	N.S.

Note.—N.S. indicates no significant difference.

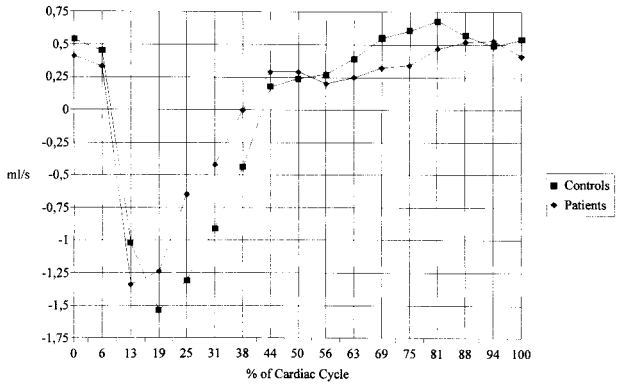

FIG. 5. Flow rates (mean values) of posterior cervical CSF motion. There are significant differences between patients and control subjects at 75% of the cardiac cycle.

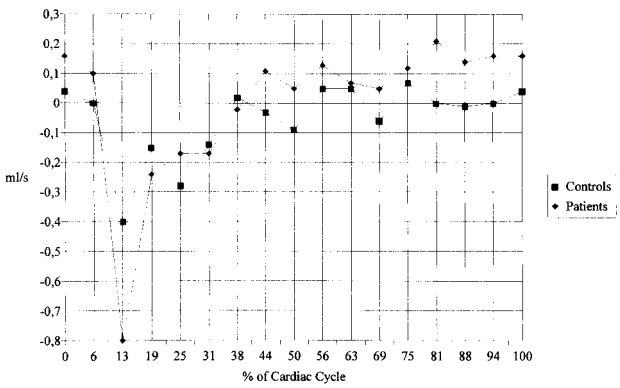

FIG. 6. Volumetric motion (mean values) of the upper cervical cord. Significant differences are seen between patients and control subjects at 69% and 81% of the cardiac cycle.

TABLE 3: Comparison of area measurements between patients with and without syrinx

Area	Syrinx	No Syrinx	Difference
Intradural space	3.8 ± 1.4 cm^2	2.5 ± 0.3 cm^2	$P < .01$
Spinal cord	1.3 ± 0.4 cm^2	0.8 ± 0.1 cm^2	$P < .01$
Anterior CSF	1.1 ± 0.7 cm^2	0.9 ± 0.1 cm^2	N.S.
Posterior CSF	1.4 ± 0.6 cm^2	0.9 ± 0.4 cm^2	$P < .05$

Note.—N.S. indicates no significant difference.

motion was significantly faster in the patients. Table 3 shows the anatomic data and Table 4 the dynamic data for our subgroups with and without syringeal formation. We found a significant increase in the cross-sectional areas of the intradural space and spinal cord in patients with syringomyelia. Patients with a syrinx tended to have a larger posterior CSF compartment. Among the dynamic data, we measured a significant increase in maximum systolic cord motion in patients with syringomyelia, whereas the subgroup without a syrinx had values within the normal range.

Discussion

With the increasingly widespread use of MR imaging over the past decade, a higher prevalence of Chiari I malformations and a richer spectrum of clinical and neuroradiologic findings have been revealed than were previously appreciated. Although a careful clinical assessment remains the cornerstone of proper diagnosis and treatment, there is no uniformity of opinion regarding the management of patients with Chiari I malformations (1). Functional examinations using dynamic MR imaging promise to provide a pathophysiologically related parameter to aid in decision making. Previous studies have consistently shown an abnormally increased pulsatile mobility of the tonsils and cord (4–6), whereas the results concerning the upper cervical CSF have been less uniform (2, 4, 6). Studies with axial imaging were therefore advocated in order to encompass all compartments of the upper spinal canal, including the lateral CSF (2).

Imaging Sequence

Phase-contrast ECG-gated multiphase sequences are the mainstay of CSF and brain motion analysis. To estimate flow velocities, the use of an imaging plane that is perpendicular to the assumed direction of flow encoding for through-slice motion is recommended. In the present study, CSF flow and spinal cord motion in the first approximation occurred perpendicular to the image plane. For such through-image flow, the product of measured velocity and ROI is the rate of flow through the ROI. This product is robust even with minor changes in the direc-

TABLE 4: Comparison of maximum volumetric flow and motion rates between patients with and without syrinx

Area	Syrinx	No Syrinx	Difference
Intradural space, systole	−4.3 ± 1.7 mL/s	−4.4 ± 1.7 mL/s	N.S.
Spinal cord, systole	−1.0 ± 0.6 mL/s	−0.5 ± 0.1 mL/s	$P < .01$
Anterior CSF, systole	−2.1 ± 0.8 mL/s	−2.8 ± 1.2 mL/s	N.S.
Posterior CSF, systole	−1.8 ± 1.0 mL/s	−1.6 ± 0.6 mL/s	N.S.
Intradural space, diastole	2.1 ± 0.8 mL/s	2.6 ± 1.5 mL/s	N.S.
Spinal cord, diastole	0.5 ± 0.2 mL/s	0.2 ± 0.2 mL/s	N.S.
Anterior CSF, diastole	1.1 ± 0.3 mL/s	1.8 ± 1.0 mL/s	N.S.
Posterior CSF, diastole	0.8 ± 0.4 mL/s	0.8 ± 0.6 mL/s	N.S.

Note.—N.S. indicates no significant difference.

tion of flow. Small vector components of motion that do not run exactly perpendicular to the plane can therefore be neglected (9).

One major advantage of the technique used is the linear relationship between phase information and first-order (constant velocity) motion (10). This concurs well with our constant flow phantom experiments. High-order motion (linear acceleration and its temporal derivatives) in the present setting, however, can be neglected: estimates have shown that phase angles per acceleration unit ($d\phi/da$) are at least one order of magnitude smaller than phase angles per velocity unit ($d\phi/dv$) (11, 12). In vivo, excellent linear correlations have been found between blood flow velocities measured with MR imaging and with Doppler sonography (13). It has to be stated, however, that phase contrast is excellent for observing laminar flow but will significantly under-represent more complex flow. This may lead to significant errors in evaluating flow in pathologic conditions inferior to the tonsillar borders in Chiari I; for example, where there are complex flow patterns.

Residual phase effects caused by eddy currents stemming from previous flow-encoding gradients can cause undesired phase shifts and false velocity measurements. These errors were effectively eliminated by subtracting from the measurement data the apparent velocity of a region with no significant motion (ie, the neck muscles).

The prospective gating strategy we applied permitted an analysis of the whole cardiac cycle. One disadvantage of prospective as opposed to retrospective gating is the increase in measurement time. Physiologic fluctuations of the heartbeat interval meant that a considerable number of trigger pulses—every other pulse on average—occurred too early to be accepted and were therefore rejected. It is also known that such variations of the heartbeat interval may blur the late (diastolic) image frames (9).

Normal Findings

Much of the MR research on spinal CSF flow and cord motion is performed using a midsagittal slice orientation (1, 14). Authors have found a pulsatile, biphasic motion of the cervical CSF: the caudal (systolic) phase starts with a delay of approximately 100 milliseconds after the R wave (corresponding to approximately 13% of a typical cardiac cycle of 800 milliseconds). Peak caudal CSF velocities occur at 130 to 175 milliseconds (16% to 22%). Occasionally, a smaller caudal CSF velocity peak is observed between 450 and 500 milliseconds (56% to 63%). CSF diastole starts with delays ranging from 300 to 500 milliseconds (38% to 63%). In the midsagittal plane, CSF flow velocities have been measured in a range from 0.7 cm/s (diastole) to −1.3 cm/s (systole). Studies based on axial slice orientation have arrived at similar results. The onset of cervical CSF systole occurs with a delay of 100 milliseconds (13%) after the R wave and lasts for about 300 milliseconds (38%). CSF diastole starts with a delay of 400 to 600 milliseconds, corresponding to 50% to 75% of the cardiac cycle (15). The flow velocities range from 0.7 cm/s at diastole to −2.3 cm/s at systole. Peripheral triggering (eg, with a finger photoplethysmograph) is one alternative to ECG triggering. A comparison of both triggering methods requires an assessment of the delay induced by peripheral gating. In peripheral triggering, the percentage of the cardiac cycle relative to the onset is defined by means of the finger pulse. This places the onset of carotid systole at approximately 60% to 70% of the cycle (16, 17). In ECG triggering, on the other hand, the onset of carotid systole occurs at 10% of the cardiac cycle (18). This constant shift of 50% to 60% has to be subtracted from the peripheral gating if the findings are to be compared with ECG gating. With sagittal slice orientation and peripheral triggering, peak craniocaudal (systolic) flow velocity was found at 65% to 88%, and peak caudocranial (diastolic) velocity occurred at 0% to 44% of the cardiac cycle. These values correspond to approximately 10% to 30% and 45% to 90%, respectively, with ECG gating. Systolic velocities anterior to the cord, at the C2–C3 disk level, were found to be -3.1 ± 1.7 cm/s, and the diastolic values were 2.1 ± 1.3 cm/s (2). With the use of a transverse slice projection and peripheral gating, peak flow ranged from −2.1 cm/s at systole to 2.3 cm/s at diastole (16). Oscillatory CSF flow volume at the level of C2–C3 was found to be 39 ± 4 mL/min, or 0.65 ± 0.07 mL/s (19).

In addition to CSF flow, upper cervical cord motion has also been studied. The onset of caudal motion in the spinal cord occurs near the end of the cephalic CSF flow period (ie, somewhere around 13%) and lasts only 50 to 70 milliseconds (6% to 9%) (17). Slightly later in CSF systole, while cervical CSF is still moving in a caudal direction, the cord starts moving cephalad. The peak systolic velocities of the cord are 0.57 ± 0.28 cm/s.

Our findings concur well with the results obtained by others. Upper cervical CSF flow followed an approximately sinusoidal pattern. Peak systolic flow occurred at approximately 20% and peak diastolic flow at 80% of the cardiac cycle. The volumetric flow rates are of the same order of magnitude as previously published data derived from a very small sample of volunteers (20, 21). The literature concerned with a quantitative analysis of upper spinal cord motion contains surprisingly few data (17, 22, 23). In our study, the spinal cord underwent a slight early systolic caudal displacement superimposed on a subtle oscillatory rather than sinusoidal motion. It is worth noting that changes in the volumetric rate of the cord alone amount to only 10% of the volume displaced in the intradural compartment as a whole. The caudal motion of the cord precedes the maximum CSF flow in the cervical subarachnoid space, occupies a much shorter time period, and terminates

while CSF is still flowing caudad. Assuming a mean cross-sectional area of the spinal cord of 0.9 cm^2, as was the case in our healthy volunteers, a peak systolic ''flow'' rate of −0.5 mL/s corresponds to a velocity of −0.6 cm/s, which accords well with previously published data (17, 22, 23). The so-called Monroe-Kellie doctrine assumes a constant intracranial volume due to the rigidity of the skull. Intracranial dynamics are the result of an interplay between the arterial blood pool, venous blood pool, brain, and CSF. Previous dynamic MR studies have shown that the arterial pulsation arriving in the cranial cavity is only temporarily accommodated in the cranium and is then ''discharged'' via CSF flow and cord motion through the foramen magnum (24). The shift of cord and CSF volumes observed in our study is approximately equivalent to the intracranial arteriovenous difference. The onset is due to arterial expansion followed by caudal motion and expansion of the brain (18).

Patients

Alterations in craniospinal brain and cord motion were discovered even before the advent of MR imaging. In a myelographic study, Du Boulay et al (25) reported pulsatile movements of the cerebellar tonsils in eight of 64 patients with Chiari I malformations and associated hydromyelia. The tonsils were observed to be thrust caudally into the cervical canal in systole and then retracted in diastole. The authors observed no such motions in control subjects.

Similarly, cine MR imaging with presaturation bolus tracking revealed increased downward displacement of the cerebellar tonsils and upper cord in all patients with Chiari I malformation (5). Upward motion, on the other hand, was reported only sporadically. A systolic downward and diastolic upward motion of the CSF anterior to the cord was observed in both patients and control subjects alike.

Most of the MR studies of the dynamics in Chiari I malformation were performed with phase-contrast techniques and based mainly on sagittal sections. The most consistent finding in patients was the increased systolic caudal movement of the cord and tonsils. This pathologic motion was very regular: the downward displacement of the tonsils started early at systole, before the intracranial arterial pulse wave, and reached its peak at 19% to 25% of the cardiac cycle (6). Wolpert et al (4) found a similar temporal relationship and increase of craniocaudal motion in the upper spinal cord. With peripheral gating, caudal displacement of the cord and tonsils started simultaneously at 70% of the cardiac cycle, corresponding to 10% to 20% with ECG gating. This concurs well with our results. We observed the beginning of caudal motion of the cord between 6% and 13% of the cardiac cycle. Despite our limited temporal resolution, our finding of a short time period in which we measured the caudal motion of the cord is in agreement with previous studies (1, 3). Nonetheless, apparent differences between our results and those of Wolpert may be explained by the better temporal precision and reliability of ECG triggering as opposed to peripheral triggering, in which varying time delays between cardiac systole and the peripheral trigger pulse probably have a blurring effect.

Previous analyses of CSF flow in Chiari I have yielded what are, in part, conflicting results. In patients with Chiari I malformations, CSF diastolic flow in the precord CSF spaces was found to precede that in the control subjects by about 15% of the cardiac cycle (4). Conversely, we found this to be the case in the posterior CSF compartment, whereas in the precord CSF the flow in our patients was slightly delayed at late systole and early diastole. Our results also contradict a quantitative analysis done with sagittal imaging of the anterior CSF compartment in which an impaired systolic and unaltered diastolic flow were measured (2). Furthermore, our results are also at variance with a previous semiquantitative report (1) in which the authors postulated an obstruction of CSF flow in Chiari patients: CSF flow velocities were decreased, periods of caudal CSF flow were shorter, and the terminal 50% of the cardiac cycle showed dampened CSF flow velocities in patients. In our patient sample, we found no significant flow obstruction at systole; yet our patients had impaired CSF flow in the second half of the cardiac cycle.

The measurements we obtained appear plausible: during systole, CSF and cord are displaced through the foramen magnum into the spinal canal. In patients with obstruction of the foramen, this spatial demand is accommodated by an increased downward displacement of the tonsils and upper spinal cord. Just why this motion of the cord is so abrupt and terminates so quickly remains unclear. One explanation could be the retracting force of the brain stem; another, the cessation of the driving force. The high amplitude of the arterial pressure wave, which necessitates instant movement, explains why the systolic displacement of the spinal canal contents is very similar in both control subjects and patients with an obstruction of the foramen magnum. At diastole, however, the retracting forces are weaker and can be modulated by plugging the tonsils in the foramen magnum. This explains why there is a significantly slower return to equilibrium in patients than in control subjects. Another hypothesis would include a different intracranial/extracranial pressure gradient in patients and control subjects. With obstructed CSF flow at the craniocervical junction, the intracranial compartment may be less compliant for incoming blood or CSF flow and this would result in changes in blood or CSF flow dynamics that should be taken into account.

The pathophysiologic mechanism of syringeal formation in Chiari I has been the subject of much speculation. Starting with Gardner's theory (3) of a ''water hammer'' effect on the central canal, no

convincing concept has so far been presented. Recent evidence suggests that syringes occurring with hindbrain lesions are not caused by caudal flow from the fourth ventricle into the central canal of the spinal cord (26). In Chiari I, the upper part of the spinal cord is usually distorted and compressed and the syringes usually extend below the constricted segment, often at some distance from the fourth ventricle. Another hypothesis suggests that increased downward pulsation of the cerebellar tonsils causes them to act as pistons on the cervical subarachnoid space, thus compressing the cord surface (3). The tonsils and spinal cord are moved into the spinal canal and can either actively convey pulsations and shearing forces, thus contributing to syringeal formation, or, alternatively, act as an obstacle to the propagation of the pulsating CSF flow waves. In view of the results of recent MR studies, increased pulsations of the spinal cord have been postulated to account for the formation of a syrinx (5). Our results lend weight to this hypothesis, as we found systolic cord motion to differ significantly in patients with and without a syrinx.

Another theory introduces the Bernoulli effect (4): the pressure in a moving liquid can be divided into the static pressure perpendicular to the direction of flow and the dynamic pressure in the flow direction. As flow velocity decreases, static pressure increases and dynamic pressure decreases. At low speeds, therefore, the static pressure exerted on the wall of a pipe must be high (27). If volumetric CSF flow, as shown in our study, is not significantly different in patients with and without a syrinx, flow velocity would have to decrease to compensate an increased cross-sectional area available for CSF flow. Our data support this concept, as patients with a syrinx tended to have a larger posterior CSF compartment.

Finally, additional unknown variables might be responsible for the formation of a syrinx. One of these factors includes a sudden rise in intradural pressure induced by Valsalva maneuvers and coughing (28). Invasive pressure recordings have shown a characteristic impairment of the return to equilibrium in patients with Chiari I malformation, in whom the system had been artificially perturbed (29).

The morphologic findings typical of Chiari I are by no means rare. In a series of 200 asymptomatic persons, one control subject was reported to have cerebellar tonsils projecting 5 mm below the foramen magnum (8). Another study found 68 patients fulfilling the diagnostic criteria in a sample of 12,226 patients who had been examined by MR imaging (30). The corresponding prevalence rates are 0.5% and 0.6%, respectively. On the other hand, one third of patients fulfilling the diagnostic criteria of Chiari I were asymptomatic. It is conceivable that a certain proportion of incidentally diagnosed subjects will eventually incur signs and symptoms related to the malformation, whereas others will continue to remain asymptomatic (31). It is commonly believed that clinical symptoms occur only when arachnoid scarring and adhesions progressively develop near the foramen magnum. The interference of such adhesions with normal CSF dynamics has therefore been implicated in the development of syringomyelia. The measurement of flow and motion on MR studies has the potential to identify a subgroup of patients who are at risk of becoming symptomatic.

In patients who already are symptomatic, whether because of brain stem or cord compression or because of syringomyelia, the correct timing of decompressive surgery is important, as is the choice of the appropriate procedure. Patients with Chiari I malformation who were symptomatic as a result of brain stem compression improved markedly after decompression. Symptoms resulting from syringomyelia, however, only stabilized or improved just slightly (31). Surgery appears to reverse the pathophysiology of progressive deterioration, and early diagnosis and treatment are critical to obtain the best outcome for the patient.

Postoperative studies after decompression mirrored the velocity profiles of healthy subjects (1). Good correlation with postoperative improvement was reported (2), which suggests that dynamic MR studies may help us understand the natural history and pathogenesis of the Chiari I malformation. So far, however, no therapeutic inferences should be drawn from flow measurements. The method and its results should rather be validated in a larger sample of patients by correlating the imaging findings with clinical symptoms and by evaluating the sensitivity and specificity of MR findings with regard to the outcome of surgical treatment.

Conclusion

Our study has shown an impairment of the passive recoil of the spinal cord and return of CSF associated with an obstruction of the foramen magnum in patients with Chiari I malformation. The increased systolic caudal motion of the cord in patients can be explained by the compensatory venting of neural structures through the foramen magnum due to the obstruction of the CSF spaces. Our results shed some light on the pathogenesis of Chiari-associated syringomyelia, as cord pulsations were increased in the subgroup of patients with syringeal formation. Further studies should not only include quantitative studies of the temporal relationship of CSF and cord motion at strategically important locations, such as the foramen magnum, the anterior and posterior spinal canal, and the cord cavities, but also the relationship of CSF dynamics to the clinical findings and results obtained after decompressive surgery.

Acknowledgment

We would like to dedicate this manuscript to Prof. Dr. M. Nadjmi on the occasion of his 70th birthday.

References

1. Armonda RA, Citrin CM, Foley KT, Ellenbogen RG. **Quantitative cine-mode magnetic resonance imaging of Chiari I malformations: an analysis of cerebrospinal fluid dynamics.** *Neurosurgery* 1994;35:214–224
2. Bhadelia RA, Bogdan AR, Wolpert SM, Lev S, Appignani BA, Heilman CB. **Cerebrospinal fluid flow waveform: analysis in patients with Chiari I malformation by means of gated phase-contrast MR imaging velocity measurements.** *Radiology* 1995; 196:195–202
3. Oldfield EH, Muraszko K, Shawker TH, Patronas NJ. **Pathophysiology of syringomyelia associated with Chiari I malformation of the cerebellar tonsils.** *J Neurosurg* 1994;80:3–15
4. Wolpert SM, Bhadelia RA, Bogdan AR, Cohen AR. **Chiari I malformations: assessment with phase-contrast velocity MR.** *AJNR Am J Neuroradiol* 1994;15:1299–1308
5. Terae S, Miyasaka K, Abe S, Abe H, Tashiro K. **Increased pulsatile movement of the hindbrain in syringomyelia associated with the Chiari malformation: cine-MR with presaturation bolus tracking.** *Neuroradiology* 1994;36:125–129
6. Pujol J, Roig C, Capdevila A, et al. **Motion of the cerebellar tonsils in Chiari type I malformation studied by cine phase-contrast MRI.** *Neurology* 1995;45:1746–1753
7. Aboulezz AO, Sartor K, Geyer CA, Gado MH. **Position of the cerebellar tonsils in the normal population and in patients with Chiari I malformation: a quantitative approach with MR imaging.** *J Comput Assist Tomogr* 1985;9:1033–1036
8. Barkovich AJ, Wippold FJ, Sherman JL, Citrin CM. **Significance of cerebellar tonsillar position on MR.** *AJNR Am J Neuroradiol* 1986;7:795–799
9. Pelc NJ, Herfkens RJ, Shimakawa A, Enzmann DR. **Phase contrast cine magnetic resonance imaging.** *Magn Reson Q* 1991;7: 229–254
10. Evans AJ, Iwai F, Grist TA, et al. **Magnetic resonance imaging of blood flow with a phase subtraction technique.** *Invest Radiol* 1993;28:109–115
11. Lingamneni A, Hardy PA, Powell KA, Pelc NJ, White RD. **Validation of cine phase-contrast MR imaging for motion analysis.** *J Magn Reson Imaging* 1995;5:331–338
12. Ståhlberg F, Mogelvang J, Thomsen C, et al. **A method for MR quantification of flow velocities in blood and CSF using interleaved gradient-echo pulse sequences.** *Magn Reson Imaging* 1989;7:655–667
13. Pelc LR, Pelc NJ, Rayhill SC, et al. **Arterial and venous blood flow: noninvasive quantitation with MR imaging.** *Radiology* 1992;185:809–812
14. Levy LM, Di Chiro G. **MR phase imaging and cerebrospinal fluid flow in the head and spine.** *Neuroradiology* 1990;32:399–406
15. Greitz D, Nordell B, Ericsson A, Ståhlberg F, Thomsen C. **Notes on the driving forces of the CSF circulation with special emphasis on the piston action of the brain.** *Neuroradiology* 1991; 33(Suppl):178–181
16. Enzmann DR, Pelc NJ. **Normal flow patterns of intracranial and spinal cerebrospinal fluid defined with phase-contrast cine MR imaging.** *Radiology* 1991;178:467–474
17. Enzmann DR, Pelc NJ. **Brain motion: measurement with phase-contrast MR imaging.** *Radiology* 1992;185:653–660
18. Greitz D, Wirestam R, Franck A, Nordell B, Thomsen C, Ståhlberg. F. **Pulsatile brain movement and associated hydrodynamics studied by magnetic resonance phase imaging.** *Neuroradiology* 1992;34:370–380
19. Enzmann DR, Pelc NJ. **Cerebrospinal fluid flow measured by phase-contrast cine MR.** *AJNR Am J Neuroradiol* 1993;14:1301–1307
20. Greitz D, Franck A, Nordell B. **On the pulsatile nature of intracranial and spinal CSF-circulation demonstrated by MR imaging.** *Acta Radiol* 1993;34:321–328
21. Greitz D, Hannertz J, Rähn T, Bolander H, Ericsson A. **MR imaging of cerebrospinal fluid dynamics in health and disease.** *Acta Radiol* 1994;35:204–211
22. Mikulis DJ, Wood ML, Zerdoner OAM, Poncelet BP. **Oscillatory motion of the normal cervical spinal cord.** *Radiology* 1994;192: 117–121
23. Tanaka H, Sakurai K, Iwasaki M, et al. **Craniocaudal motion velocity in the cervical spinal cord in degenerative disease as shown by MR imaging.** *Acta Radiol* 1997;38:803–809
24. Alperin N, Vikingstad EM, Gomez-Anson B, Levin DN. **Hemodynamically independent analysis of cerebrospinal fluid and brain motion observed with dynamic phase contrast MRI.** *Magn Reson Med* 1996;35:741–754
25. Du Boulay G, Shah SH, Currie JC, Logue V. **The mechanism of hydromyelia in Chiari type I malformations.** *Br J Radiol* 1974; 47:579–584
26. Milhorat T, Miller JI, Johnson WD, Adler DE, Heger IM. **Anatomical basis of syringomyelia occurring with hindbrain lesions.** *Neurosurgery* 1993;32:748–754
27. Resnick R, Halliday D, Krane KS. *Physics* vol 1, 4th ed. New York: Wiley; 1992: 397–405
28. Morgan D, Williams B. **Syringobulbia: a surgical appraisal.** *J Neurol Neurosurg Psychiatry* 1992;55:1132–1141
29. Williams B. **Simultaneous cerebral and spinal fluid pressure recordings, 2: cerebrospinal dissociation with lesions at the foramen magnum.** *Acta Neurochir* 1981;59:123–142
30. Elster AD, Chen MM. **Chiari I malformations: clinical and radiologic reappraisal.** *Radiology* 1992;183:347–353
31. Bindal AK, Dunsker SB, Tew JM. **Chiari I malformation: classification and management.** *Neurosurgery* 1995;37:1069–1074